HHS Public Access

Author manuscript

J Vis Exp. Author manuscript; available in PMC 2019 July 02.

A Mouse Model to Assess Innate Immune Response to *Staphylococcus aureus* Infection

Leif S. Anderson[1], **Mack B. Reynolds**[1], **Kathryn R. Rivara**[1], **Lloyd S. Miller**[2], and **Scott I. Simon**[1]

[1]Department of Biomedical Engineering, University of California Davis

[2]Department of Dermatology, Johns Hopkins University School of Medicine

Abstract

Staphylococcus aureus (*S. aureus*) infections, including methicillin resistant stains, are an enormous burden on the healthcare system. With incidence rates of *S. aureus* infection climbing annually, there is a demand for additional research in its pathogenicity. Animal models of infectious disease advance our understanding of the host-pathogen response and lead to the development of effective therapeutics. Neutrophils play a primary role in the innate immune response that controls *S. aureus* infections by forming an abscess to wall off the infection and facilitate bacterial clearance; the number of neutrophils that infiltrate an *S. aureus* skin infection often correlates with disease outcome. LysM-EGFP mice, which possess the enhanced green fluorescent protein (EGFP) inserted in the Lysozyme M (LysM) promoter region (expressed primarily by neutrophils), when used in conjunction with in vivo whole animal fluorescence imaging (FLI) provide a means of quantifying neutrophil emigration noninvasively and longitudinally into wounded skin. When combined with a bioluminescent *S. aureus* strain and sequential in vivo whole animal bioluminescent imaging (BLI), it is possible to longitudinally monitor both the neutrophil recruitment dynamics and in vivo bacterial burden at the site of infection in anesthetized mice from onset of infection to resolution or death. Mice are more resistant to a number of virulence factors produced by *S. aureus* that facilitate effective colonization and infection in humans. Immunodeficient mice provide a more sensitive animal model to examine persistent *S. aureus* infections and the ability of therapeutics to boost innate immune responses. Herein, we characterize responses in LysM-EGFP mice that have been bred to MyD88-deficient mice (LysM-EGFP×MyD88$^{-/-}$ mice) along with wild-type LysM-EGFP mice to investigate *S. aureus* skin wound infection. Multispectral simultaneous detection enabled study of neutrophil recruitment dynamics by using in vivo FLI, bacterial burden by using in vivo BLI, and wound healing longitudinally and noninvasively over time.

Keywords

Immunology and Infection; Issue 144; Staphylococcus aureus; innate immunity; neutrophils; wound healing; inflammation; whole-animal imaging

Correspondence to: Scott I. Simon at sisimon@ucdavis.edu.

Video Link

The video component of this article can be found at https://www.jove.com/video/59015/

Introduction

Staphylococcus aureus (*S.* aureus) accounts for the majority of skin and soft tissue infections (SSTIs) in the United States[1]. The incidence of methicillin-resistant *S. aureus* (MRSA) infections has increased steadily over the past two decades[2], motivating the study of the mechanisms of persistence and the discovery of new treatment strategies. The standard of care for MRSA infections is systemic antibiotic therapy, but MRSA has become increasingly resistant to antibiotics over time[3] and these drugs can diminish the host's beneficial microbiome, causing negative health effects, especially in children[4]. Preclinical studies have examined alternative strategies to treat MRSA infections[5], but translating these approaches to the clinic has proved challenging due to emergence of virulence factors that thwart host immune responses[6]. To dissect the host- pathogen dynamics that drive *S. aureus* SSTIs, we combine noninvasive and longitudinal readouts of the number of neutrophils recruited to the wound bed with kinetic measures of bacterial abundance and wound area.

Neutrophils are the most abundant circulating leukocyte in humans and the first responders to a bacterial infection[7]. Neutrophils are a necessary component for an effective host response against *S. aureus* infections due to their bactericidal mechanisms, including production of reactive oxygen species, proteases, antimicrobial peptides and functional responses including phagocytosis and neutrophil extracellular trap production[8,9]. Human patients with genetic defects in neutrophil function, such as chronic granulomatous disease and Chediak-Higashi syndrome, show an increased susceptibility to *S. aureus* infection. In addition, patients with genetic (such as congenital neutropenia) and acquired (such as neutropenia seen in chemotherapy patients) defects in neutrophil numbers are also highly susceptible to *S. aureus* infection[10]. Given the importance of neutrophils in clearing *S. aureus* infections, enhancing their immune capacity or tuning their numbers within a *S. aureus* lesion may prove an effective strategy in resolving infection.

Over the past decade, transgenic mice with fluorescence neutrophil reporters have been developed to study their trafficking[11,12]. Combining neutrophil reporter mice with whole animal imaging techniques permits spatiotemporal analysis of neutrophils in tissues and organs. When combined with bioluminescent strains of *S. aureus*, it is possible to track the accumulation of neutrophils in response to *S. aureus* abundance and persistence in the context of bacterial virulence factors that directly and indirectly perturb neutrophil numbers in affected tissue[13,14,15,16].

Mice are less susceptible to *S. aureus* virulence and immune evasion mechanisms than humans. As such, wild-type mice may not be an ideal animal model to investigate the efficacy of a given therapeutic to treat chronic *S. aureus* infection. MyD88-deficient mice (i.e., MyD88$^{-/-}$ mice), an immunocompromised mouse strain that lacks functional interleukin-1 receptor (IL-1R) and Toll-like receptor (TLR) signaling, show greater susceptibility to *S. aureus* infection compared to wild-type mice[17] and an impairment in neutrophil trafficking to a site of *S. aureus* infection in the skin[18]. Development of a mouse strain that possesses a fluorescent neutrophil reporter in MyD88$^{-/-}$ mice has provided an

alternative model for investigating the efficacy of therapies to treat *S. aureus* infection compared to current neutrophil reporter mice.

In this protocol, we characterize *S. aureus* infection in the immunocompromised LysM-EGFP×MyD88$^{-/-}$ mice, and compare the time course and resolution of infection with the LysM-EGFP mice. LysM-EGFP×MyD88$^{-/-}$ mice develop a chronic infection that does not resolve, and 75% succumb to infection after 8 days. A significant defect in initial neutrophil recruitment occurs over 72 h of the inflammatory phase of infection, and 50% fewer neutrophils recruit during the latter stage of infection. The increased susceptibility of the LysM-EGFP×MyD88$^{-/-}$ mice makes this particular strain a rigorous preclinical model to evaluate the efficacy of new therapeutic techniques targeting *S. aureus* infection compared to current models that utilize wild-type mice, especially techniques aiming to boost the innate immune response against infection.

Protocol

All mouse studies were reviewed and approved by the Institutional Animal Care and Use Committee at UC Davis and were performed according to the guidelines of the Animal Welfare Act and the Health Research Extension Act. Be sure to use sterile gloves when working with animals.

1. Mouse Source and Housing

1. Derive LysM-eGFP mice on a C57BL/6J genetic background as described previously[12]. Derive LysM-EGFP×MyD88$^{-/-}$ mice by crossing LysM- EGFP mice with MyD88$^{-/-}$ mice on a C57BL/6J background.
2. House mice in a vivarium. For these studies, animals were housed at the University of California, Davis in groups prior to surgery and single housed following surgery. Use mice between the ages of 10–16 weeks.

2. Bacterial Preparation and Quantification

1. Remove the bioluminescent *S. aureus* strain of interest from −80 °C storage to thaw on ice. Streak on a 5% bovine blood agar plate. Incubate the streaked plate in a humidified incubator at 37 °C overnight (16 h).

   NOTE: In this protocol, the ALC2906 SH1000 strain was used. This strain contains the shuttle plasmid pSK236 with the penicillin-binding protein 2 promoter fused to the *luxABCDE* reporter cassette from *Photohabdus luminescens*[18].
2. Prepare tryptic soy broth (TSB) by mixing 0.03 g of TSB powder per mL of pure water, and autoclave TSB to sterilize. When cooled, add any necessary antibiotics using sterile technique. In this protocol, add 10 μg/mL of chloramphenicol[18] to the TSB to select for expression of the pSK236 shuttle plasmid, which contains the bioluminescence luxABCDE cassette.

3. Pick 3–4 separate colonies from the *S. aureus* plate into TSB with 10 μg/mL chloramphenicol to start an overnight culture. Incubate bacteria on an incubating shaker at 37 °C overnight (16 h).

4. Start a new bacterial culture from the overnight culture by diluting a sample 1:50 into TSB with 10 g/mL chloramphenicol. Culture in an incubating shaker at 200 rpm and 37 °C.

5. Two hours after splitting the *S. aureus*, monitor the optical density at 600 nm (OD_{600}) on a spectrophotometer. Observe the OD_{600} vs. time to find mid-logarithmic phase growth. For the ALC2906 SH1000 strain, an OD_{600} of 0.5 is mid-logarithmic and corresponds to a concentration of 1×10^8 CFU/mL (Figure 1).

6. When OD_{600} is 0.5, wash bacteria 1:1 with ice-cold DPBS. Centrifuge the bacteria for 10 min at 3,000 × *g* and 4 °C. Carefully decant the supernatant and add additional chilled DPBS and vortex thoroughly. Centrifuge once more for 10 min at 3,000 × *g* and 4 °C.

7. Carefully decant the supernatant. Resuspend the bacterial pellet at a desired concentration. For these studies, collect 3 mL of ALC2906 SH1000 and resuspend in 1.5 mL of PBS, correlating to a bacteria concentration of about 2×10^8 CFU/mL. Keep bacteria on ice until use.

8. To verify bacteria concentration, dilute 100 μL of the bacterial sample 1:10,000 and 1:100,000 in PBS. Plate 20 μ L aliquots on an agar plate. Incubate at 37 °C in a humidified incubator for 16 h. Count CFUs by gross examination and calculate a bacterial concentration the following day.

3. Excisional Skin Wounding and Inoculation with *S. aureus*

1. Administer 100 μ L of 0.03 mg/mL buprenorphine hydrochloride (~0.2 mg/kg) to each mouse *via* intraperitoneal injection.

2. Twenty minutes post-injection, place 2–4 mice in a chamber with 2–3 LPM oxygen with 2–4% isoflurane. Once mice are fully anesthetized, transfer the mice one at a time to a nose cone connected to 2–3 LPM oxygen with 2–4% isoflurane. Verify mice are fully anesthetized by firmly pinching each rear paw between a thumb and forefinger. Proceed to the next step if the animal does not respond to the pinch.

3. Shave a 1 inch by 2 inch section on the back of the mouse with electric clippers and clear the area of fur clippings using a clean wipe or gauze. Avoid using depilatory lotion because it may cause excess inflammation.

4. Clean the back of the mouse first with 10% povidone-iodine soaked gauze and then with a 70% ethanol soaked gauze. Clean the area in a spiral pattern, moving outward from the center of the surgical area. Wait approximately 1 min for the surgical area to dry prior to surgery.

5. Hold the shaved back of the mouse loosely between two fingers and firmly press a sterile 6 mm punch biopsy at the center of the prepared surgical area. Do not pull the skin taut.
    1. Twist the punch biopsy to create a circular outline on the skin that fully cuts through the skin in at least one section of the outline. Be careful not to cut into the underlying fascia or tissue.
    2. Use sterile scissors and forceps to cut through the epidermis and dermis following the circular pattern imprinted by the punch biopsy.

4. *S.* aureus Inoculation

1. Fill a 28 G insulin syringe with the desired bioluminescent bacterial inoculant. In this study, administer a concentration of 1×10^8 CFU/mL (50 µL). Do not administer more than 100 µL of volume.
2. Inject 50 µL of inoculant between the fascia and tissue in the center of the wound on the back of the mouse. Ensure that the inoculant forms a bubble at the center of the wound with minimal leakage or dispersion.
    1. Pull the dermis to the side, hold the syringe nearly parallel to the tissue, and slowly push the syringe into the tissue until a sudden decrease in resistance is felt, which indicates piercing of the fascia. Carefully lead the syringe into the center of the wound and dispense the inoculant slowly. Remove the syringe slowly from the animal.
3. Inject the same volume of sterile PBS into the wounds of uninfected animals as described above.
4. Return the animal to its cage. Place the cage under a heat lamp or on top of a heating pad, and monitor the animal until recovery from anesthesia.

5. In Vivo BLI and FLI

1. Initialize the whole animal imager through the instrument software. Anesthetize mice in a chamber receiving 2–3 LPM oxygen with 2–4% isoflurane. Deliver anesthesia to the nosecones inside the imager.
2. Place the wounded and infected mouse into the imager. Position the mouse such that the wound is as flat as possible. Use the following sequence set-up to image the mice.
    1. Select **Luminescence** and **Photograph** as the imaging mode. The exposure time is 1 min at small binning and F/stop 1 (luminescence) and F/stop 8 (photograph). The emission filter is **Open**. Click the **Acquire** button to record the image.
    2. Select **Fluorescence** and **Photograph** as the imaging mode. The exposure time is 1 s at small binning and F/stop 1 (Fluorescence) and F/stop 8 (photograph) with an excitation wavelength of 465/30 nm and an

emission wavelength 520/20 nm with a high lamp intensity. Click the **Acquire** button to record the image.

3. Return the animal to its cage and monitor until recovery from anesthesia.

4. Image mice daily as described above.

6. Image Analysis

1. Open images to be quantified.

2. Place a large circular region of interest (ROI) over the entire wound area including surrounding skin for each mouse in the image. The neutrophil in vivo FLI EGFP signals and in vivo BLI *S. aureus* signals extend beyond the wound edge after several days and were included in these studies (Figure 2A and 2B). Click **Measure ROI** and record values for mean flux for each mouse. Plot the mean flux of each signal (p/s) *versus* time.

3. If absolute numbers of neutrophils or *S. aureus* in the wound are desired, perform the following experiments.

    1. To correlate neutrophil numbers to the in vivo FLI EGFP signals, wound C57BL/6J mice as described above, and transfer a range of bone marrow-derived neutrophils (5×10^5 to 1×10^7) from LysM-EGFP or LysM-EGFPxMyD88$^{-/-}$ donors directly on top of different wounds. Image as described above and correlate the in vivo FLI EGFP signals to the known quantity of neutrophils.

    2. To correlate *S. aureus* CFU to the in vivo BLI signals, wound and infect mice as described above. On day 1 post-infection record in vivo BLI signals from the mice and immediately euthanize and chill carcasses. Excise the wound, homogenize the tissue, and plate bacterial dilutions on agar for overnight incubation. The next day, count colonies to determine CFU per wound.

4. To measure wound healing fit a circular ROI over the wound edge and measure the area of the wound (cm^2) and plot the fractional change from baseline vs. time (Figure 2C).

7. Statistics

NOTE: All data are presented as mean ±SEM. $p < 0.05$ were considered statistically significant

1. Determine differences between two groups on a single day using the Holm-Sidak method, with alpha = 0.05, and analyze each time point individually, without assuming a consistent SD.

2. Compare differences between multiple groups on the same day by one-way ANOVA with the Tukey multiple-comparisons posttest. Survival between experimental groups was analyzed by the Mantel-Cox method.

Representative Results

LysM-EGFP×MyD88$^{-/-}$ mice are more susceptible to *S. aureus* infection than LysM-EGFP mice

The strain of *S. aureus* used in this study, ALC2906[18], was constructed with a plasmid that contains the *lux* construct that produces bioluminescent signals from live and actively metabolizing bacteria. When inoculated into mice, in vivo bioluminescence imaging (BLI) techniques can be used to longitudinally measure bacteria burden within an infected wound. Both LysM-EGFP×MyD88$^{-/-}$ mice and LysM-EGFP mice were wounded and infected with 1×10^7 CFU of *S. aureus* in the wound to compare their susceptibility to *S. aureus* infection. LysM- EGFP×MyD88$^{-/-}$ mice showed greater susceptibility to infection than LysM-EGFP mice demonstrated by 80% lethality of LysM-EGFP×MyD88$^{-/-}$ mice during the first 8 days of infection compared to 0% lethality of LysM-EGFP mice during the entire 15-day duration of the experiment (Figure 3A). Both strains of mice lost ~5% body weight following infection, but LysM-EGFP mice recovered original weight by day 2, while LysM-EGFP×MyD88$^{-/-}$ mice did not recover lost weight (Figure 3B). Wound closure in the presence of *S. aureus* infection was not different between the two strains; however, sterilely wounded LysM-EGFP×MyD88$^{-/-}$ had a significant defect in wound healing compared to LysM-EGFP mice (Figure 3C), as previously reported[19]. Whole animal imaging was used to measure bacterial burden daily, and as early as day 1, LysM- EGFP×MyD88$^{-/-}$ wounds had a higher bacterial burden than LysM-EGFP wounds. LysM-EGFP mice controlled infection and decreased in vivo BLI signals in the wound, while LysM-EGFP×MyD88$^{-/-}$ mice exhibited an increase in bacterial burden that plateaued on day 4 until animal death (Figure 3D,E). Together, these data demonstrate the increased susceptibility of LysM-EGFP×MyD88$^{-/-}$ mice to *S. aureus* infection compared to LysM-EGFP mice.

Neutrophil trafficking is impaired in *S. aureus* infected LysM-EGFP×MyD88$^{-/-}$ mice compared to LysM-EGFP mice

The LysM-EGFP mouse produces green fluorescent neutrophils due to a EGFP protein encoded downstream of the Lysozyme M promoter[12]. This mouse has been utilized to study longitudinal in vivo neutrophil trafficking in response to dermal *S. aureus* infection[13,14,20,21,22]. To compare neutrophil kinetics to wounds produced on LysM-EGFP and LysM-EGFP×MyD88$^{-/-}$ mice, a 6 mm full thickness skin wound was administered on the dorsum, and mice were imaged daily. A 40% decrease in neutrophil trafficking to wounds was observed in LysM-EGFP×MyD88$^{-/-}$ compared to LysM-EGFP mice (Figure 4A,C). When 1×10^7 CFU of *S. aureus* was introduced immediately after wounding, neutrophil trafficking was attenuated in both strains of mice, but LysM-EGFP×MyD88$^{-/-}$ mice were more sensitive to *S. aureus* infection with respect to neutrophil recruitment. Infection caused a 50% decrease in initial neutrophil trafficking to LysM-EGFP×MyD88$^{-/-}$ wounds compared to a 15% decrease observed in LysM-EGFP wounds (Figure 4B). LysM-EGFP mice also recruited significantly more neutrophils to the wound during the later stages of infection (Figure 4A,C) compared to LysM-EGFP×MyD88$^{-/-}$ mice, which were unable to increase neutrophil numbers even in the presence of sustained bacterial burden. Together, these data demonstrate that LysM-EGFP×MyD88$^{-/-}$ mice have a defect in neutrophil recruitment, which is consistent with their increased susceptibility to *S. aureus* infection.

Discussion

S. aureus infection models that utilize bioluminescent *S. aureus* infection in a fluorescent neutrophil reporter mouse in conjunction with advanced techniques of whole animal in vivo optical imaging have advanced our knowledge of the innate immune response to infection. Previous studies using the LysM-EGFP mouse have shown that up to 1×10^7 neutrophils recruit to an *S. aureus* infected wound over the first 24 h of infection[14], and wound-recruited neutrophils extend their half-life from 1.5 days to 5 days in response to a *S. aureus*-infected wound[22]. A survival tactic adapted by mice to combat infection is trafficking of hematopoietic stem and progenitor cells (HSPC) to an infected wound from the bone marrow where they expand into bactericidal $EGFP^+$ neutrophils in a TLR2/MyD88/PGE_2 dependent manner[21]. In addition, extramedullary granulopoiesis provides an essential source of neutrophils to rescue *S. aureus* infected $MyD88^{-/-}$ mice from lethal sepsis[13]. Adoptive transfer of HSPC from LysM-EGFP mice into wild type mice makes it possible to examine the process of local neutrophil production and its importance in combatting *S. aureus* within a wound[13,21]. It is also possible to calibrate precisely the number of neutrophils in the wound; neutrophil number in wounds correlates linearly with EGFP signal from 1×10^6 to greater than 1×10^7 neutrophils, and the limit of detection is about 1×10^6 neutrophils in a 6 mm wound[14].

In our representative results we compare longitudinal neutrophil and *S. aureus* kinetics in the wounds of LysM-EGFP and LysM- EGFP×$MyD88^{-/-}$. To our knowledge, this is this first study that compares the bacterial burden and neutrophil trafficking between wild type and immunocompromised mice longitudinally through resolution of infection. Of particular interest is the degree of neutrophil recruitment attenuation caused by *S. aureus* infection in the $MyD88^{-/-}$ strain, which elicited a 15% decrease in neutrophil trafficking in wild type mice compared to a 50% decrease in $MyD88^{-/-}$. *S. aureus* is able to evade the host's immune response by producing a number of virulence factors known to indirectly inhibit neutrophil trafficking (i.e., α-toxin, Panton-Valentine leukocidin, and Chemotaxis inhibitory protein[23,24]), and our results indicate that MyD88 signaling, likely through TLR2, TLR4, and IL-1R, is critical to overcome the strategies employed by S. aureus to evade host immune responses. Virulence factor-knockout *S. aureus* strains can be used in this model to characterize their effect on myeloid cell trafficking[13]. Further, when studied in conjunction with the LysM-EGFP×$MyD88^{-/-}$ mouse, this model highlights the role of MyD88 signaling in combatting the pathogenic effects of virulence factors.

There are several critical steps in this protocol that if performed improperly can introduce variability into studies. The wounding and infection procedures are straightforward compared to other mouse disease models, but it is not without its intricacies. Skin punch biopsies are very sharp and can easily cut into the spinotrapezius muscle below the skin. Damaging this muscle and its fascia alters neutrophil recruitment and increases variability between mice and a results in a more invasive *S. aureus* infection that is not centered within the wound. Mice with significant damage to the spinotrapezius muscle should be excluded from studies.

Another source of error in this model comes from changes in the bioluminescent *S. aureus* strain over time, which can alter in vivo BLI signals and growth kinetics. The ALC2906 strain contains a shuttle plasmid that contains the modified *lux* operon from *Photorhabdus luminescens* construct that is required to produce the bioluminescent signals, which can be discarded by the *S. aureus* bacteria over time[25]. In a broth culture without selection, 97% of SH1000 colonies produced bioluminescent signals on day 3. This frequency dropped to 53% on day 5 and 21% on day 10[26]. Thus, at later time points during the infectious course, the in vivo BLI signals will likely begin to slightly (<1 log difference) underestimate the actual *in vivo* bacterial burden. It is important to freeze down fresh glycerol stocks of *S. aureus* with antibiotic selection to maintain the plasmid upon arrival and replacing working stocks of bacteria frequently (i.e., every three months) can help prevent loss of the bioluminescent construct during culture maintenance. Newer strains of bioluminescent *S. aureus* contain a stably integrated bioluminescent construct[27,28] and are likely an improvement over the ALC2906 strain used in this model.

While this model is useful to study localized dermal *S. aureus* infections, it has limitations. The in vivo BLI signals of bacterial burden is limited to the wound and adjacent skin. The model does not provide a reliable readout for deep invasive infections such as sepsis, and animals must be euthanized to measure dissemination of bacteria in to the bloodstream or kidneys[13]. Newer and brighter engineered bioluminescent strains have been generated that can permit the detection of in vivo BLI signals from internal organs[27,28]. In addition, longitudinal detection and monitoring of neutrophil trafficking cannot be measured in other commonly acquired *S. aureus* infections, including respiratory and blood infections. Reduced sensitivity due to tissue autofluorescence is also a limitation of this model. The recently developed Catchup mouse utilizes a TdTomato RFP under the Ly6G promoter and may have a higher signal to noise ratio than the LysM-EGFP mouse due to reduced tissue auto fluorescence in the RFP channel[11].

The potential crosstalk between in vivo BLI and FLI emission signals in this model is worthy of discussion but is negligible. If we perform experiments without light excitation and only collect in vivo FLI EGFP signals using the 520/20 filter, we do not observe any appreciable signals from infected mice, demonstrating that collected signals are from in vivo FLI EGFP signals and not from overlap of in vivo BLI signals of the bacteria (data not shown). This is primarily due to the signal collection time, which is only 1 second for in vivo FLI and 1 minute for in vivo BLI, and a specific excitation wavelength filter of 465/30 nm and emission filter of 520/20 nm. These settings allow for optimal detection of in vivo FLI EGFP signals without contribution from in vivo BLI signals. This is best demonstrated when comparing the order of magnitude of the y-axis between Figure 3D and Figure 4A. The signals from the in vivo BLI is about 100-fold less than the in vivo FLI of EGFP signals, indicating that the in vivo BLI signals are negligible and contribute to less than 1% of the signals observed from in vivo FLI.

We expect future applications of this model will help researchers discover and characterize *S. aureus* virulence factors, and serve as a pre- clinical animal model to test novel therapeutics that aim to clear *S. aureus* infection by boosting the innate immune response.

Acknowledgments

This work was supported by National Institutes of Health Grants R01 AI129302 (to S.I.S.) and the Training Program in Pharmacology: From Bench to Bedside at UC Davis (NIH T32 GM099608 to L.S.A). The Molecular and Genomic Imaging (CMGI) at the University of California Davis provided superb technological support.

Disclosures

Lloyd S. Miller has received grant support from MedImmune, Pfizer, Regeneron, and the Chan Soon-Shiong Nanthealth Foundation and consulting fees from Noveome Biotherapeutics and the Chan Soon-Shiong Nanthealth Foundation that are unrelated to the work reported in this paper. The other authors have nothing to disclose.

References

1. Moran GJ et al. Methicillin-Resistant S. aureus Infections among Patients in the Emergency Department. New England Journal of Medicine. 355 (7), 666–674 (2009).
2. Suaya JA et al. Incidence and cost of hospitalizations associated with Staphylococcus aureus skin and soft tissue infections in the United States from 2001 through 2009. BMC Infectious Diseases. 14 (1), 296 (2014). [PubMed: 24889406]
3. Ventola CL The antibiotic resistance crisis: part 1: causes and threats. P & T: a Peer-Reviewed Journal for Formulary Management. 40 (4), 277–283 (2015). [PubMed: 25859123]
4. Blaser MJ Antibiotic use and its consequences for the normal microbiome. Science. 352 (6285), 544–545 (2016). [PubMed: 27126037]
5. Hilliard JJ et al. Anti-Alpha-Toxin Monoclonal Antibody and Antibiotic Combination Therapy Improves Disease Outcome and Accelerates Healing in a Staphylococcus aureus Dermonecrosis Model. Antimicrobial Agents and Chemotherapy. 59 (1), 299–309 (2015). [PubMed: 25348518]
6. Proctor RA Recent developments for Staphylococcus aureus vaccines: clinical and basic science challenges. European Cells & Materials. 30, 315–326 (2015). [PubMed: 26629971]
7. Mölne L, Verdrengh M, & Tarkowski A Role of Neutrophil Leukocytes in Cutaneous Infection Caused by Staphylococcus aureus. Infection and Immunity. 68 (11), 6162–6167 (2000). [PubMed: 11035720]
8. Kolaczkowska E, & Kubes P Neutrophil recruitment and function in health and inflammation. Nature Reviews Immunology. 13 (3), 159–175 (2013).
9. Borregaard N Neutrophils, from Marrow to Microbes. Immunity. 33 (5), 657–670 (2010). [PubMed: 21094463]
10. Miller LS, & Cho JS Immunity against Staphylococcus aureus cutaneous infections. Nature Reviews Immunology. 11 (8), 505–518 (2011).
11. Hasenberg A et al. Catchup: a mouse model for imaging-based tracking and modulation of neutrophil granulocytes. Nature Methods. 12 (5), 445–452 (2015). [PubMed: 25775045]
12. Faust N, Varas F, Kelly LM, Heck S, & Graf T Insertion of enhanced green fluorescent protein into the lysozyme gene creates mice with green fluorescent granulocytes and macrophages. Blood. 96 (2), 719–726 (2000). [PubMed: 10887140]
13. Falahee PC et al. α-Toxin Regulates Local Granulocyte Expansion from Hematopoietic Stem and Progenitor Cells in Staphylococcus aureus-Infected Wounds. Journal of immunology (Baltimore, Md.: 1950). 199 (5), 1772–1782 (2017).
14. Kim M-H et al. Dynamics of Neutrophil Infiltration during Cutaneous Wound Healing and Infection Using Fluorescence Imaging. Journal of Investigative Dermatology. 128 (7), 1812–1820 (2008). [PubMed: 18185533]
15. Liese J, Rooijakkers SHM, Strijp JAG, Novick RP, & Dustin ML Intravital two-photon microscopy of host-pathogen interactions in a mouse model of Staphylococcus aureus skin abscess formation. Cellular Microbiology. 15 (6), 891–09 (2013). [PubMed: 23217115]
16. Bogoslowski A, Butcher EC, & Kubes P Neutrophils recruited through high endothelial venules of the lymph nodes *via* PNAd intercept disseminating Staphylococcus aureus. Proceedings of the National Academy of Sciences of the United States of America. 115 (10), 2449–2454 (2018). [PubMed: 29378967]

17. Takeuchi O, Hoshino K, & Akira S Cutting Edge: TLR2-Deficient and MyD88-Deficient Mice Are Highly Susceptible to Staphylococcus aureus Infection. The Journal of Immunology. 165 (10), 5392–5396 (2000). [PubMed: 11067888]

18. Miller LS et al. MyD88 Mediates Neutrophil Recruitment Initiated by IL-1R but Not TLR2 Activation in Immunity against Staphylococcus aureus. Immunity. 24 (1), 79–91 (2006). [PubMed: 16413925]

19. Macedo L et al. Wound healing is impaired in MyD88-deficient mice: a role for MyD88 in the regulation of wound healing by adenosine A2A receptors. The American Journal of Pathology. 171 (6), 1774–1788 (2007). [PubMed: 17974599]

20. Cho JS et al. Neutrophil-derived IL-1β Is Sufficient for Abscess Formation in Immunity against Staphylococcus aureus in Mice. PLoS Pathogens. 8 (11), e1003047 (2012). [PubMed: 23209417]

21. Granick JL et al. Staphylococcus aureus recognition by hematopoietic stem and progenitor cells *via* TLR2/MyD88/PGE2 stimulates granulopoiesis in wounds. Blood. 122 (10), 1770–1778 (2013). [PubMed: 23869087]

22. Kim MH et al. Neutrophil survival and c-kit+-progenitor proliferation in Staphylococcus aureus-infected skin wounds promote resolution. Blood. 117 (12), 3343–3352 (2011). [PubMed: 21278352]

23. Foster TJ Immune evasion by staphylococci. Nature Reviews Microbiology. 3 (12), 948–958 (2005). [PubMed: 16322743]

24. Gordon RJ, & Lowy FD Pathogenesis of Methicillin-Resistant Staphylococcus aureus Infection. Clinical Infectious Diseases. 46 (Supplement_5), S350–S359 (2008). [PubMed: 18462090]

25. Cho JS et al. Neutrophil-derived IL-1β Is Sufficient for Abscess Formation in Immunity against Staphylococcus aureus in Mice. PLoS Pathogens. 8 (11), e1003047–20 (2012). [PubMed: 23209417]

26. Bernthal NM et al. A mouse model of post-arthroplasty Staphylococcus aureus joint infection to evaluate *in vivo* the efficacy of antimicrobial implant coatings. PLoS ONE. 5 (9), e12580 (2010). [PubMed: 20830204]

27. Plaut RD, Mocca CP, Prabhakara R, Merkel TJ, & Stibitz S Stably Luminescent Staphylococcus aureus Clinical Strains for Use in Bioluminescent Imaging. PLoS ONE. 8 (3), e59232 (2013). [PubMed: 23555002]

28. Dillen CA et al. Clonally expanded γδ T cells protect against Staphylococcus aureus skin reinfection. The Journal of Clinical Investigation. 128 (3), 1026–1042 (2018). [PubMed: 29400698]

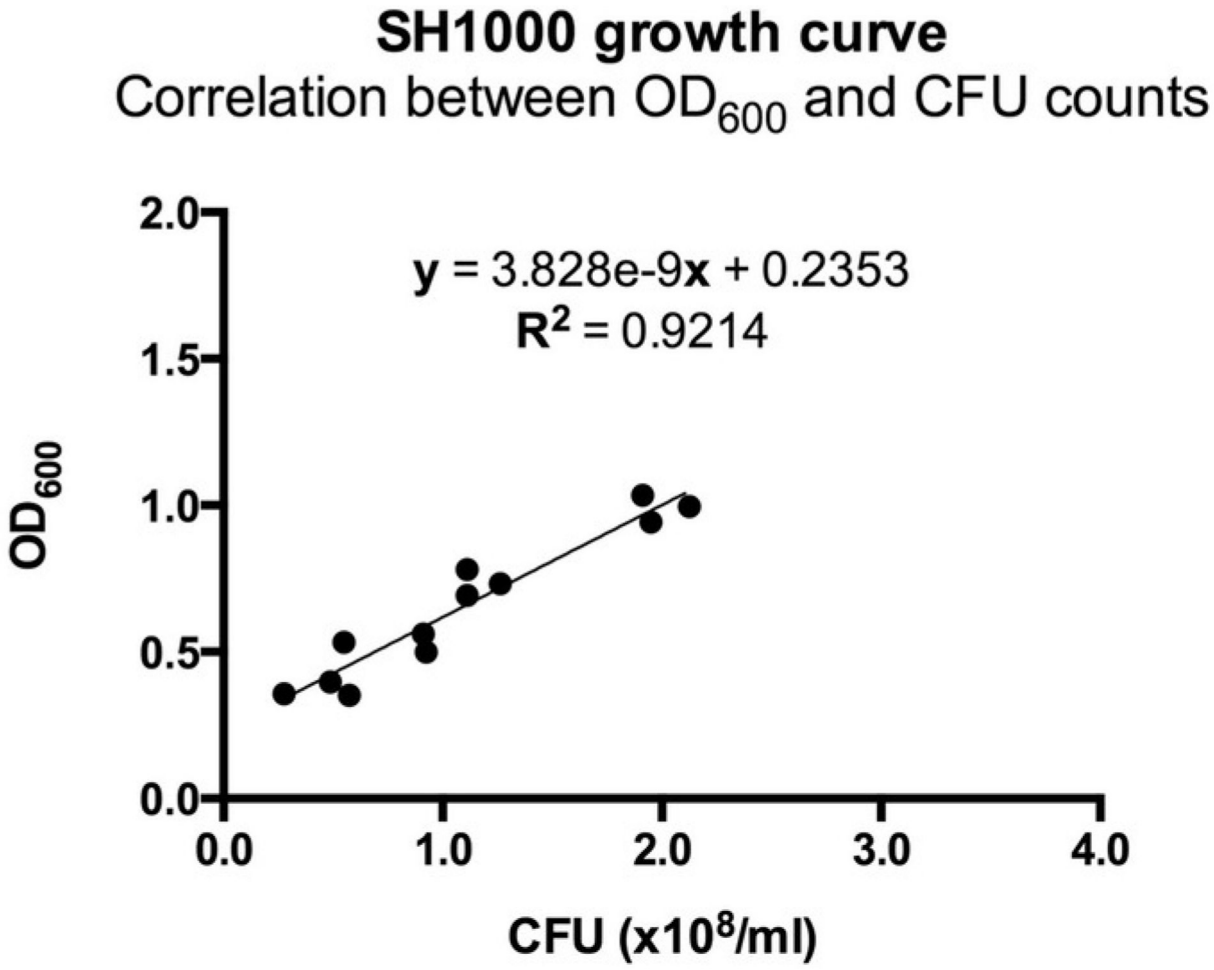

Figure 1: Correlation between OD_{600} and CFU counts for ALC2906.

3–4 ALC2906 SH1000 colonies were picked from an agar plate and transferred into TSB with 10 μg/mL chloramphenicol for overnight culture. The next day, the suspension was split 1:50 into TSB with 10 μg/mL chloramphenicol and cultured. Optical density at 600 nm (OD_{600}) was measured in regular intervals after 2 hours using a spectrophotometer.At each measurement the bacteria was diluted 1:100,000 in ice cold PBS and aliquoted onto an agar plate for overnight incubation. CFUs were counted the following day to calculate the initial concentration and correlated to OD_{600}. N = 3 with 4 different OD_{600} measurements per experiment.

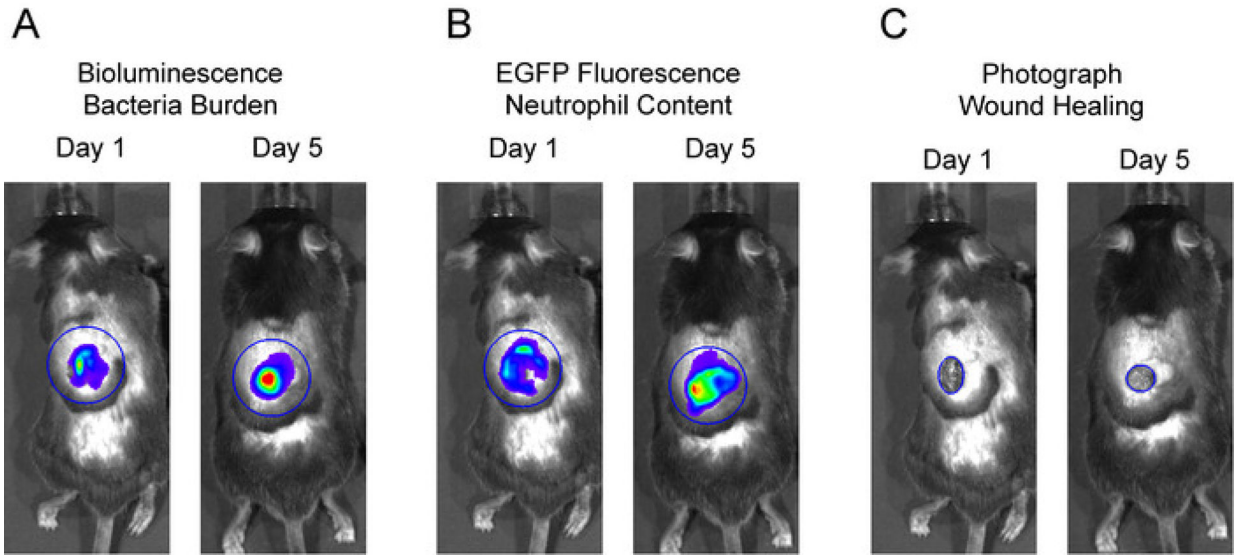

Figure 2: Representative region of interests (ROIs) for data analysis.

To analyze in vivo BLI and in vivo FLI signals, large, equivalent sized ROIs were centered over the wound and total flux (photons per second) was measured. To measure wound closure, an ROI was fit to the wound edge and area (cm^2) was measured.

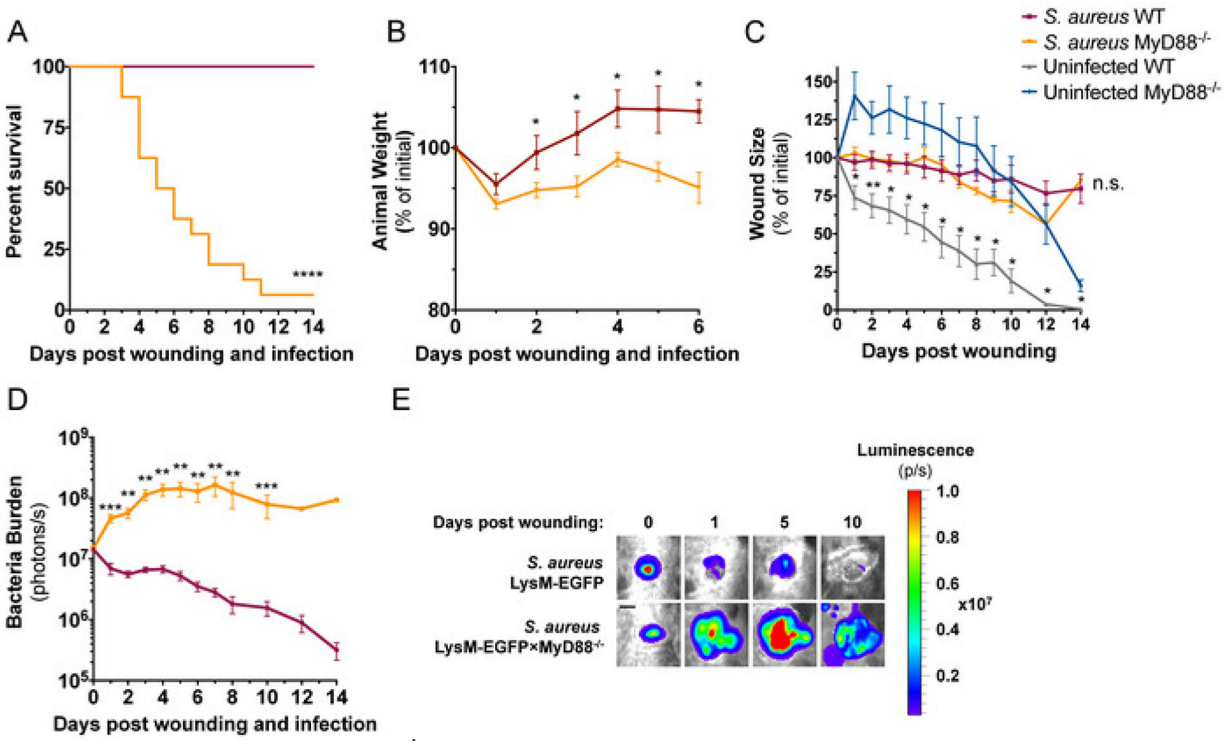

Figure 3: LysM-EGFP×MyD88$^{-/-}$ mice are more susceptible to *S. aureus* infection compared to LysM-EGFP mice.

LysM-EGFP and LysM- EGFP×MyD88$^{-/-}$ mice were administered a 6 mm wound on the dorsum and infected with 1 × 10^7 CFU of bioluminescent *S. aureus* or sterile saline. Animals were monitored daily and (**A**) survival and (**B**) weight were recorded. Animals were imaged daily to measure (**C**) wound size and (**D**) bacterial luminescence. (**E**) Representative bioluminescent images are depicted from infected LysM-EGFP and LysM-EGFP×MyD88$^{-/-}$ mice.Scale bar = 3 mm. Data represent 7–16 mice per group for A, C, and D and 3 mice per group for B and are expressed as mean ±SEM. * $p = 0.05$, ** $p = 0.01$, *** $p = 0.001$, **** $p < 0.0001$ between infected (**A, B,** and **D**) or uninfected (**C**) groups. Statistical significance was determined using Mantel-Cox test (**A**) and the Holm-Sidak method (**B-D**), with alpha = 0.05, and each time point was analyzed individually, without assuming a consistent SD.

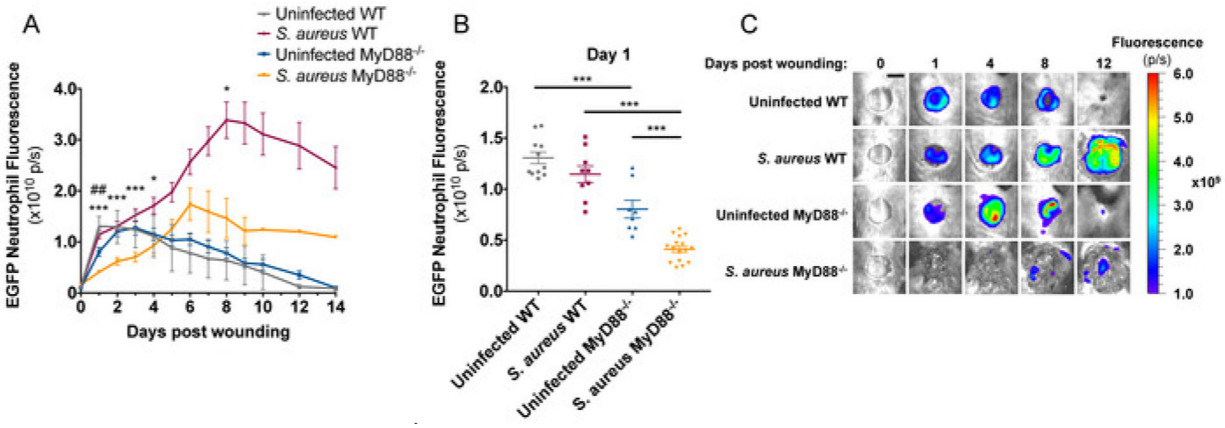

Figure 4: LysM-EGFP×MyD88$^{-/-}$ mice have defective neutrophil recruitment to infected wounds.

LysM-EGFP and LysM-EGFP×MyD88$^{-/-}$mice were administered a 6mm wound on the dorsum and infected with 1 × 10^7 CFU of bioluminescent *S. aureus* or sterile saline. Animals were imaged daily to measure (**A,B**) neutrophil content. (**C**) Representative fluorescent images are depicted from infected and non-infected LysM-EGFP and LysM-EGFP×MyD88$^{-/-}$ mice. Scale bar = 5 mm. Data represent 8–16 mice per group and are expressed as mean ±SEM. *p < 0.05, ** $p < 0.01$, and *** $p < 0.001$ between infected groups and$^{\#\#}$ $p < 0.01$ between uninfected groups (**A**) or as depicted on the graph (**B**). Statistical significance was determined using the Holm-Sidak method (**A**), with alpha = 0.05, and each time point was analyzed individually, without assuming a consistent SD, and one-way ANOVA (**B**), with the Tukey multiple-comparisons post-test.